

## Aromatic–Aromatic Interactions Induce the Self-Assembly of Pentapeptidic Derivatives in Water To Form Nanofibers and Supramolecular Hydrogels

Manlung Ma,<sup>†,‡</sup> Yi Kuang,<sup>†</sup> Yuan Gao,<sup>†</sup> Yan Zhang,<sup>‡</sup> Ping Gao,<sup>§</sup> and Bing Xu<sup>\*,†,‡</sup>

*Department of Chemistry, Brandeis University, Waltham, Massachusetts 02454, and Departments of Chemistry and of Chemical and Biomolecular Engineering, The Hong Kong University of Science and Technology, Clear Water Bay, Hong Kong, China*

Received October 17, 2009; E-mail: bxu@brandeis.edu

**Abstract:** In this paper we report the conjugation of an aromatic moiety (pyrene (**P**), fluorene (**F**), or naphthalene (**N**)) to pentapeptides GAGAS (**1**), GVPVP (**2**), VPGVG (**3**), VTEEI (**4**), VYGGG (**5**), and YGFGG (**6**) to afford peptidic derivatives for exploring pentapeptide-based hydrogels as potential biomaterials. Most of these compounds (**1F**, **1P**, **2F**, **2P**, **4F**, **4P**, **4N**, **5F**, **5N**, **6F**, **6P**, and **6N**) behave as molecular hydrogelators and can form hydrogels at minimum concentrations of gelation from 0.5 to 2.8 wt %. The fluorescence spectra of the hydrogels exhibit a significant red shift, indicating the interactions between the aromatic moieties in those hydrogels. The circular dichroism spectra indicate that the self-assembly of the hydrogelators affords helical or  $\beta$ -sheet-like structures. Transmission and scanning electron microscopic examination reveals the nanofiber networks of these hydrogelators. In addition, rheological measurements show fair to excellent viscoelastic properties of these hydrogels. The balance of intermolecular aromatic–aromatic interactions and hydrogen bonds of these hydrogelators leads to their self-assembly in water and the formation of nanofibers as the matrixes of hydrogels. A total of 6 of these 18 pentapeptide derivatives—**1N**, **2N**, **3F**, **3P**, **3N**, and **5P**—fail to form hydrogels under the conditions tested, likely due to unbalanced intermolecular interactions. This work suggests that aromatic–aromatic interactions are useful and favorable forces for creating molecular nanofibers and supramolecular hydrogels.

### Introduction

In this paper we report the evaluation of a series of pentapeptidic derivatives to elucidate the minimum structural prerequisites and driving forces of a molecule containing a pentapeptidic motif to act as a hydrogelator.<sup>1–4</sup> Composed of three-dimensional, elastic networks and a liquid in their interstitial spaces, gels possess many useful properties, such as forming hierarchical structures, flowing in response to a shear force,<sup>5</sup> and exhibiting phase transitions upon other stimuli such

as a change in temperature,<sup>6</sup> ligand–receptor interaction,<sup>7</sup> variation of the pH value,<sup>8</sup> enzymatic conversion,<sup>9</sup> and irradiation of light.<sup>10</sup> Gels have found applications in many areas including biocatalysis,<sup>11</sup> bioanalysis,<sup>12</sup> chemical sensing,<sup>13</sup> food processing,<sup>14</sup> cosmetics,<sup>15</sup> lubrication,<sup>16</sup> drug delivery,<sup>17</sup> tissue engineering,<sup>18,19</sup> wound healing,<sup>20</sup> and controlling the fate of

<sup>†</sup> Brandeis University.

<sup>‡</sup> Department of Chemistry, The Hong Kong University of Science and Technology.

<sup>§</sup> Department of Chemical and Biomolecular Engineering, The Hong Kong University of Science and Technology.

(1) Terech, P.; Weiss, R. G. *Chem. Rev.* **1997**, *97*, 3133–3159.

(2) (a) Linton, B.; Hamilton, A. D. *Chem. Rev.* **1997**, *97*, 1669–1680. (b) Jayawarna, V.; Ali, M.; Jowitt, T. A.; Miller, A. E.; Saiani, A.; Gough, J. E.; Ulijn, R. V. *Adv. Mater.* **2006**, *18*, 611–614. (c) Mart, R. J.; Osborne, R. D.; Stevens, M. M.; Ulijn, R. V. *Soft Matter* **2006**, *2*, 822–835. (d) Toledano, S.; Williams, R. J.; Jayawarna, V.; Ulijn, R. V. *J. Am. Chem. Soc.* **2006**, *128*, 1070–1071. (e) Yang, Z. M.; Liang, G. L.; Xu, B. *Chem. Commun.* **2006**, 738–740. (f) Gao, Y.; Kuang, Y.; Guo, Z. F.; Guo, Z. H.; Krauss, I. J.; Xu, B. *J. Am. Chem. Soc.* **2009**, *131*, 13576–13577.

(3) Estroff, L. A.; Hamilton, A. D. *Chem. Rev.* **2004**, *104*, 1201–1217. (4) Yang, Z. M.; Liang, G. L.; Xu, B. *Acc. Chem. Res.* **2008**, *41*, 315–326.

(5) Yoshinobu, M.; Morita, M.; Sakata, I. *J. Appl. Polym. Sci.* **1992**, *45*, 805–812.

(6) Yoshida, R.; Uchida, K.; Kaneko, Y.; Sakai, K.; Kikuchi, A.; Sakurai, Y.; Okano, T. *Nature* **1995**, *374*, 240–242.

(7) Zhang, Y.; Gu, H. W.; Yang, Z. M.; Xu, B. *J. Am. Chem. Soc.* **2003**, *125*, 13680–13681.

(8) Torres-Lugo, M.; Peppas, N. A. *Macromolecules* **1999**, *32*, 6646–6651.

(9) (a) Yang, Z. M.; Gu, H. W.; Fu, D. G.; Gao, P.; Lam, J. K.; Xu, B. *Adv. Mater.* **2004**, *16*, 1440. (b) Yang, Z. M.; Liang, G. L.; Wang, L.; Bing, X. *J. Am. Chem. Soc.* **2006**, *128*, 3038–3043.

(10) Haines, L. A.; Rajagopal, K.; Ozbas, B.; Salick, D. A.; Pochan, D. J.; Schneider, J. P. *J. Am. Chem. Soc.* **2005**, *127*, 17025–17029.

(11) Plieva, F. M.; Kochetkov, K. A.; Singh, I.; Parmar, V. S.; Belokon, Y. N.; Lozinsky, V. I. *Biotechnol. Lett.* **2000**, *22*, 551–554.

(12) Moorthy, J.; Mensing, G. A.; Kim, D.; Mohanty, S.; Eddington, D. T.; Tepp, W. H.; Johnson, E. A.; Beebe, D. J. *Electrophoresis* **2004**, *25*, 1705–1713.

(13) (a) Holtz, J. H.; Asher, S. A. *Nature* **1997**, *389*, 829–832. Sangeetha, N. M.; Maitra, U. *Chem. Soc. Rev.* **2005**, *34*, 821–836. (b) Chen, J.; McNeil, A. J. *J. Am. Chem. Soc.* **2008**, *130*, 16496–16497.

(14) Ladet, S.; David, L.; Domard, A. *Nature* **2008**, *452*, 76–U76.

(15) Jennings, V.; Gysler, A.; Schafer-Korting, M.; Gohla, S. H. *Eur. J. Pharm. Biopharm.* **2000**, *49*, 211–218.

(16) Freeman, M. E.; Furey, M. J.; Love, B. J.; Hampton, J. M. *Wear* **2000**, *241*, 129–135. Gong, J. P. *Soft Matter* **2006**, *2*, 544–552.

(17) (a) Langer, R. *Science* **1990**, *249*, 1527–1533. (b) Langer, R. *Nature* **1998**, *392*, 5–10.

(18) Langer, R.; Vacanti, J. P. *Science* **1993**, *260*, 920–926.

cells.<sup>21</sup> In the area of bioengineering and drug delivery, most of hydrogels result from cross-linked natural or synthetic polymers,<sup>22</sup> which serve as the networks for encapsulating water and therapeutic agents. In addition, the elastin-like polypeptides have attracted numerous interest as smart biomaterials for drug release,<sup>23</sup> as temperature responsive protein pores,<sup>24</sup> as molecular switches, and as purification tools for recombinant protein expression.<sup>25</sup>

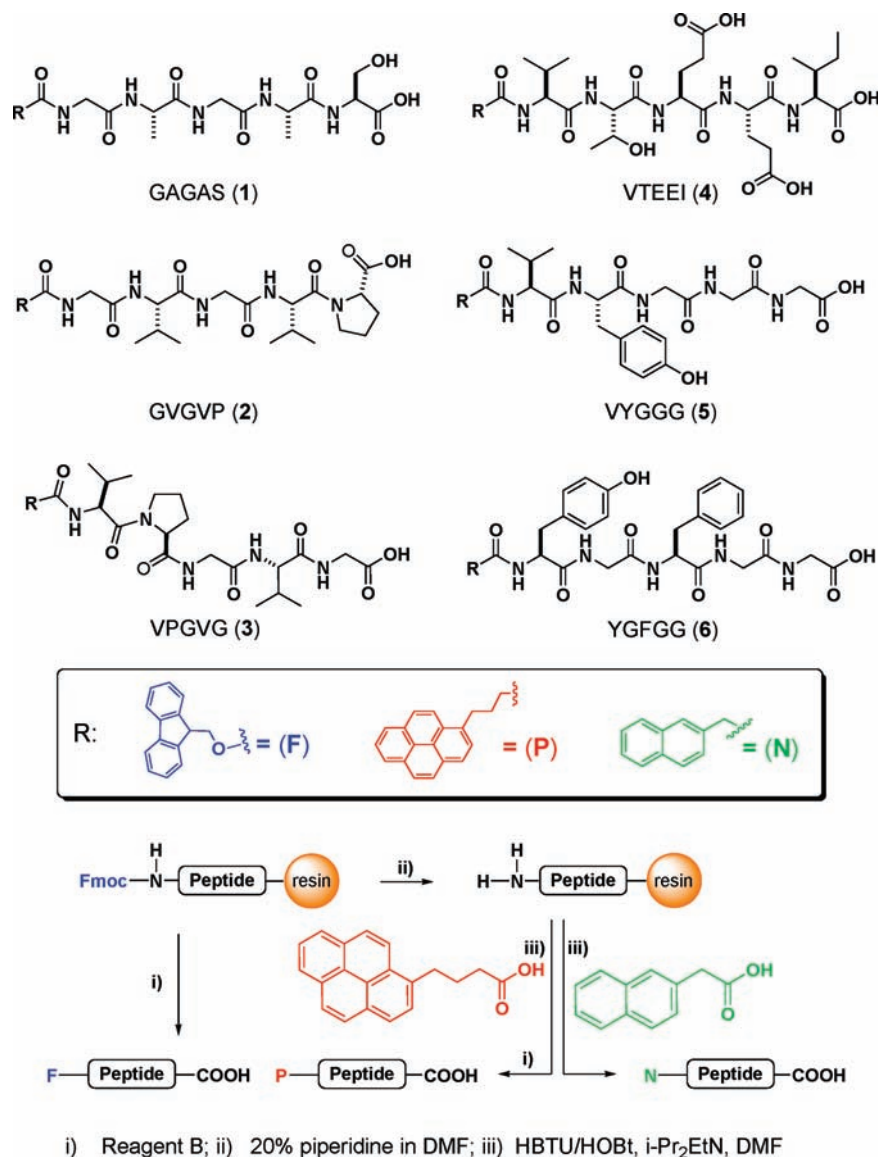
Although they received less attention previously, small or low molecular weight gelators can self-assemble to form supramolecular polymers or aggregates, whose entanglement affords the network to result in gels of organic solvents<sup>1,26</sup> or water.<sup>3,4</sup> In the past decade, the research field of the nonpolymeric (or small-molecule) gelators has experienced rapid growth. Initially, the research of low molecular weight (LMW) organogelators, which self-assemble to form nanofibers and result in organogels, advanced considerably.<sup>1,27</sup> Then small molecules that can form a gel with water re-emerged.<sup>3,28,29</sup> The demonstration of self-assembled oligopeptides, which self-assemble into nanofibers to form matrixes for encapsulating water, provides a new type of hydrogels for biomedical applications (e.g., neuron regeneration,<sup>19</sup> biomineralization,<sup>30,31</sup> and cell culturing<sup>32</sup>), which has greatly inspired the recent research efforts on low molecular weight hydrogelators.<sup>28,33</sup>

Despite the increased research and rapid advances in making and characterizing small-molecule gelators, the understanding of the structural requirements for a molecule to form a gel with a liquid remains insufficient.<sup>34</sup> While many hydrogelators bear hydrophobic alkyl chains,<sup>3</sup> which are analogous to the hydrophobic tails of natural phospholipids, only a small number of

hydrogelators consist of aromatic moieties and rely on aromatic–aromatic interactions to promote hydrogelation.<sup>35,41</sup> Compared to alkyl chains, aromatic–aromatic interactions possess several distinct merits: (i) Aromatic–aromatic interaction normally is stronger than the van der Waals interaction (London dispersion force) between alkyl chains, and it has been well-established as a stabilizing force for proteins.<sup>36</sup> Aromatic–aromatic interaction should allow the formation of more stable supramolecular polymers, thus resulting in mechanically strong or stable hydrogels. (ii) Aromatic rings have relatively compact volumes, which reduce the steric repulsion usually associated with the bulky and long alkyl chains. (iii) The overlap between aromatic rings normally adopts a plane-to-plane or an edge-to-plane orientation,<sup>36</sup> which leads to more predictable and efficient self-assembly of the molecules in either the organic or aqueous phase. To obtain the qualitative correlations, we chose to study the gelation of pentapeptidic derivatives because pentapeptides are a common motif of the epitope(s) that dictates the biological function of proteins.<sup>37</sup> Understanding and controlling the self-assembly of pentapeptides may lead to a new type of biomaterials (in the form of hydrogels, nanofibers, or micelles) that mimic and regulate biological nanostructures.<sup>38,39</sup>

Encouraged by the promising prospects of oligopeptide-based hydrogels demonstrated in recent works,<sup>19,30,39–42</sup> we chose to investigate the supramolecular hydrogels based on six pentapeptidic sequences (Scheme 1). Some sequences of these pentapeptides act as the repetitive epitopes in antigens or other biomacromolecules. For example, pentapeptide VTEEI is the repeat sequence from the *Plasmodium falciparum* blood stage antigen Pf332 recognized by certain parasite-neutralizing antibodies,<sup>43</sup> sequences GVGVP and VPGVG are short, elastin-like peptides and the epitopes found frequently in elastin,<sup>44</sup> and VYGGG exhibits an inhibitory effect in the binding monoclonal antibody 10D11.<sup>45</sup> These pentapeptides are selected in a random

- (19) Silva, G. A.; Czeisler, S.; Niece, K. L.; Beniash, E.; Harrington, D. A.; Kessler, J. A.; Stupp, S. I. *Science* **2004**, *303*, 1352–1355.
- (20) Yang, Z. M.; Liang, G. L.; Ma, M. L.; Abbah, A. S.; Lu, W. W.; Xu, B. *Chem. Commun.* **2007**, 843–845.
- (21) (a) Yang, Z. M.; Xu, K. M.; Guo, Z. F.; Guo, Z. H.; Xu, B. *Adv. Mater.* **2007**, *19*, 3152–3156. (b) Yang, Z.; Liang, G.; Guo, Z.; Guo, Z.; Xu, B. *Angew. Chem., Int. Ed.* **2007**, *46*, 8216–8219.
- (22) (a) Wu, X. S.; Hoffman, A. S.; Yager, P. J. *Polym. Sci., Part A: Polym. Chem.* **1992**, *30*, 2121–2129. (b) Park, T. G.; Hoffman, A. S. *Macromolecules* **1993**, *26*, 5045–5048. (c) Wang, C.; Stewart, R. J.; Kopecek, J. *Nature* **1999**, *397*, 417–420.
- (23) (a) Herrero-Vanrell, R.; Rincon, A. C.; Alonso, M.; Reboto, V.; Molina-Martinez, I. T.; Rodriguez-Cabello, J. C. *J. Controlled Release* **2005**, *102*, 113–122. (b) Massodi, I.; Bidwell, G. L.; Raucher, D. *J. Controlled Release* **2005**, *108*, 396–408.
- (24) Jung, Y.; Bayley, H.; Movileanu, L. *J. Am. Chem. Soc.* **2006**, *128*, 15332–15340.
- (25) Lim, D. W.; Trabbic-Carlson, K.; MacKay, J. A.; Chilkoti, A. *Biomacromolecules* **2007**, *8*, 1417–1424.
- (26) Bhattacharya, S.; Acharya, S. N. *G. Chem. Mater.* **1999**, *11*, 3121–3132.
- (27) (a) de Loos, M.; van Esch, J.; Stokroos, I.; Kellogg, R. M.; Feringa, B. L. *J. Am. Chem. Soc.* **1997**, *119*, 12675–12676. (b) Hanabusa, K.; Tanaka, R.; Suzuki, M.; Kimura, M.; Shirai, H. *Adv. Mater.* **1997**, *9*, 1095–1097. (c) Abdallah, D. J.; Weiss, R. G. *Adv. Mater.* **2000**, *12*, 1237–1247. (d) Tam, A. Y. Y.; Wong, K. M. C.; Yam, V. W. W. *J. Am. Chem. Soc.* **2009**, *131*, 6253–6260.
- (28) Estroff, L. A.; Hamilton, A. D. *Angew. Chem., Int. Ed.* **2000**, *39*, 3447+.
- (29) Menger, F. M.; Caran, K. L. *J. Am. Chem. Soc.* **2000**, *122*, 11679–11691.
- (30) Hartgerink, J. D.; Beniash, E.; Stupp, S. I. *Science* **2001**, *294*, 1684–1688.
- (31) Song, J.; Saiz, E.; Bertozzi, C. R. *J. Am. Chem. Soc.* **2003**, *125*, 1236–1243.
- (32) Bokhari, M. A.; Akay, G.; Zhang, S. G.; Birch, M. A. *Biomaterials* **2005**, *26*, 5198–5208.
- (33) (a) Kiyonaka, S.; Sugiyasu, K.; Shinkai, S.; Hamachi, I. *J. Am. Chem. Soc.* **2002**, *124*, 10954–10955. (b) Kiyonaka, S.; Shinkai, S.; Hamachi, H. *Chem.—Eur. J.* **2003**, *9*, 976–983.
- (34) George, M.; Weiss, R. G. *Acc. Chem. Res.* **2006**, *39*, 489–497.
- (35) (a) Menger, F. M.; Portnoy, C. E. *J. Am. Chem. Soc.* **1967**, *89*, 4698–4701. (b) Menger, F. M. *Acc. Chem. Res.* **1979**, *12*, 111–114. (c) Gazit, E. *FASEB J.* **2002**, *16*, 77–83. (d) Reches, M.; Gazit, E. *Science* **2003**, *300*, 625–627. (e) Valery, C.; Paternostre, M.; Robert, B.; Gulik-Krzywicki, T.; Narayanan, T.; Dedieu, J. C.; Keller, G.; Torres, M. L.; Cherif-Cheikh, R.; Calvo, P.; Artzner, F. *Proc. Natl. Acad. Sci. U.S.A.* **2003**, *100*, 10258–10262. (f) Jayawarna, V.; Ali, M.; Jowitt, T. A.; Miller, A. E.; Saiani, A.; Gough, J. E.; Ulijn, R. V. *Adv. Mater.* **2006**, *18*, 611+.
- (36) (g) Yang, Z. M.; Liang, G. L.; Ma, M. L.; Gao, Y.; Xu, B. *J. Mater. Chem.* **2007**, *17*, 850–854.
- (37) Burley, S. K.; Petsko, G. A. *Science* **1985**, *229*, 23–28.
- (38) (a) Urry, D. W. *Angew. Chem., Int. Ed. Engl.* **1993**, *32*, 819–841. (b) Panitch, A.; Yamaoka, T.; Fournier, M. J.; Mason, T. L.; Tirrell, D. A. *Macromolecules* **1999**, *32*, 1701–1703. (c) Lee, K. Y.; Mooney, D. J. *Chem. Rev.* **2001**, *101*, 1869–1879.
- (39) (a) Vauthey, S.; Santoso, S.; Gong, H. Y.; Watson, N.; Zhang, S. G. *Proc. Natl. Acad. Sci. U.S.A.* **2002**, *99*, 5355–5360. (b) Zhang, S. G.; Yan, L.; Altman, M.; Lasse, M.; Nugent, H.; Frankel, F.; Lauffenburger, D. A.; Whitesides, G. M.; Rich, A. *Biomaterials* **1999**, *20*, 1213–1220. (c) Capito, R. M.; Azevedo, H. S.; Velichko, Y. S.; Mata, A.; Stupp, S. I. *Science* **2008**, *319*, 1812–1816.
- (40) Hsu, L.; Cvetanovich, G. L.; Stupp, S. I. *J. Am. Chem. Soc.* **2008**, *130*, 3892–3899.
- (41) Holmes, T. C.; de Lacalle, S.; Su, X.; Liu, G. S.; Rich, A.; Zhang, S. G. *Proc. Natl. Acad. Sci. U.S.A.* **2000**, *97*, 6728–6733.
- (42) Xing, B. G.; Yu, C. W.; Chow, K. H.; Ho, P. L.; Fu, D. G.; Xu, B. *J. Am. Chem. Soc.* **2002**, *124*, 14846–14847.
- (43) Zhang, S. G. *Nat. Biotechnol.* **2003**, *21*, 1171–1178. (b) Rajagopal, K.; Schneider, J. P. *Curr. Opin. Struct. Biol.* **2004**, *14*, 480–486. (c) Zhang, Y.; Yang, Z. M.; Yuan, F.; Gu, H. W.; Gao, P.; Xu, B. *J. Am. Chem. Soc.* **2004**, *126*, 15028–15029.
- (44) Vasconcelos, N. M.; Siddique, A.; Ahlberg, N.; Berzins, K. *Vaccine* **2004**, *23*, 343–352.

**Scheme 1.** Chemical Structures and Synthesis of Different Pentapeptide Epitopes To Attach on a Fluorenyl, Pyrenyl, or Naphthyl Group

way to evaluate the generality of the aromatic–aromatic interaction for promoting self-assembly in water and hydrogelation.

We chose three kinds of aromatic moieties, pyrene (**P**), fluorene (**F**), and naphthalene (**N**), to covalently attach to pentapeptides GAGAS (**1**), GVPVP (**2**), VPGVG (**3**), VTEEI (**4**), VYGGG (**5**), and YGFGG (**6**). In their native forms, without the attachment of any groups at either the N-termini or the C-termini of the six different types of pentapeptides, none of these pentapeptides act as hydrogelators.<sup>46</sup> The proper balance of intermolecular aromatic–aromatic interactions and hydrogen bonds of these molecules result in molecular self-assembly in

water, which afford the networks of nanofibers and lead to hydrogelation. A total of 12 of these 18 peptidic derivatives behave as small-molecule hydrogelators and afford hydrogels at a minimum gelation concentration of less than 2.8 wt %. A total of 4 of these 18 pentapeptides—**3F**, **3P**, **3N**, and **5P**—only form precipitates upon cooling their solution from around 70 °C to room temperature. **2N** melts and forms an oily layer separating from water, and **1N** only results in a clear solution instead of a hydrogel.

The fluorescence spectra of the hydrogels and their corresponding solutions indicate that aromatic–aromatic interactions among the fluorenyl, pyrenyl, and naphthyl rings play a significant role for hydrogelation, the circular dichroism spectra show helical structure and/or  $\beta$ -sheet-like features in the hydrogels formed by the self-assembly of these pentapeptidic derivatives, and the transmission electron microscopy (TEM) and scanning electron microscopy (SEM) images indicate the presence of networks of the nanofiber of these hydrogelators in the hydrogels. Some of the hydrogels also exhibit excellent mechanical properties as demonstrated by the rheological study of these hydrogels. Our results suggest that the well-balanced

- (44) (a) Foster, J. A.; Bruenger, E.; Gray, W. R.; Sandberg, L. B. *J. Biol. Chem.* **1973**, *248*, 2876–2879. (b) Venkatachalam, C. M.; Urry, D. W. *Macromolecules* **1981**, *14*, 1225–1229. (c) McPherson, D. T.; Xu, J.; Urry, D. W. *Protein Expression Purif.* **1996**, *7*, 51–57. (d) Li, B.; Alonso, D. O. V.; Daggett, V. *J. Mol. Biol.* **2001**, *305*, 581–592. (e) Mithieux, S. M.; Weiss, A. S. *Fibrous Proteins: Coiled-Coils, Collagen and Elastomers*; Academic Press: New York, 2005; Vol. 70.
- (45) Burgess, K.; Han, I.; Zhang, A.; Zheng, W. H.; Shanmugam, K.; Featherstone, M. S.; Saragovi, H. U. *J. Pept. Res.* **2001**, *57*, 68–76.
- (46) See the Supporting Information.



hydrophobicity and hydrophilicity of the small-molecule hydrogelators in water, the strong interactions (i.e., aromatic–aromatic interactions or other noncovalent interaction) between the pentapeptidic chains of the hydrogelators, and the evenly distributed nanofibers contribute to the observed excellent mechanical property. As proved by the rheology test, **1F**, **1P**, **4F**, **4P**, and **4N** exhibit an excellent mechanical property compared with other pentapeptidic hydrogelators in this work. These results indicate that the combination of aromatic–aromatic interaction and hydrogen bonding provides a general and useful methodology to understand and explore molecular self-assembly in water for designing supramolecular nanomaterials.

## Results and Discussion

**Synthesis.** As shown in Scheme 1, all the pentapeptides were prepared by solid-phase peptide synthesis (SPPS) using 2-chlorotriethylamine resin and the corresponding N<sup>α</sup>-Fmoc-protected amino acids with side chains properly protected by a *tert*-butyl group. Followed by the removal of the Fmoc group, the first amino acid was loaded onto the resin at the C-terminal. After the resins were treated with 20% piperidine to remove the protecting group, the next Fmoc-protected amino acid was coupled to the free amino group using *O*-(benzotriazol-1-yl)-*N,N,N',N'*-tetramethyluronium hexafluorophosphate/1-hydroxybenzotriazole (HBTU/HOBt)<sup>46</sup> as the coupling reagent. The growth of the peptide chain followed the established Fmoc SPPS protocol.<sup>47</sup> Each process was monitored by a Kaiser test<sup>46</sup> or chloranil test<sup>46</sup> during the cleavage of the protecting group or the loading of an amino acid. At the final step, the N-termini of the pentapeptides were either protected by Fmoc or coupled with 1-pyrenebutyric acid or 2-naphthaleneacetic acid to attach the aromatic group (fluorenyl, pyrenyl, or naphthyl group) to the pentapeptides.

**Gelation Properties.** Because the pentapeptidic derivatives prepared in this work possess the carboxylic acid, a change of pH (deprotonation or protonation) is able to trigger hydrogelation. Table 1 shows the optical images of the hydrogels of these pentapeptidic derivatives. Most of the compounds (shown in Scheme 1) are able to form hydrogels at a certain pH and temperature (Table S-1, Supporting Information<sup>46</sup>). When the pH values are higher than the listed values in Table S-1, the hydrogels transform into clear solutions (i.e., gel–sol transition). The general procedure for making the hydrogels in this work is to dissolve the pentapeptide derivatives at a high pH solution (deprotonating the carboxylic acid) and then to lower the pH of the solution to trigger hydrogelation. Therefore, the pentapeptidic derivatives can only self-assemble and gel with water at a certain range of pH and ionic strength, similar to the mechanism of the hydrogelation of other amphiphilic oligopeptides.<sup>30,40</sup>

GAGAS, the epitope consisting of the least amount of bulk side chains, appears to be quite hydrophilic, as indicated by the fact that **1N** is soluble in water even under low pH (<3.0) and at high concentration (6.0 wt %). Bearing more hydrophobic and larger aromatic rings than the naphthyl group, **1F** and **1P** are hydrogelators that form hydrogels in an acidic condition (pH < 3) at minimum concentrations of 1 wt % and 0.5 wt %, respectively.

GVGVP, with relatively large side chains of the valine residue and a proline residue at the end of the backbone of the

**Table 1.** Optical Images of the Hydrogels of the Pentapeptide Derivatives

	(P)	(F)	(N)
GAGAS			--
GVGVP			--
VPGVG	--	--	--
VTEEI			
VYGGG	--		
YGFGG			

pentapeptide, shows poor solubility in water.<sup>48,49</sup> Carefully adjusting the pH of the solution to 4.8 results in the hydrogel of **2F**. Compound **2F** melts to become an oil above 70 °C and remains separated from the aqueous phase even after the sample is cooled back to room temperature, indicating that the proline residue at the end of the pentapeptide likely hinders efficient molecular packing. Compound **2N** either dissolves in water at pH higher than 4.0 or becomes a suspension at pH lower than <2.5. Upon heating, it also melts and becomes an oil that separates from water. This result indicates that proline is a poor candidate to serve as a residue for the backbone of this type of hydrogelators. Such an observation is supported by the fact that none of the three compounds containing VPGVG (as the pentapeptide segment) form a hydrogel at all the conditions we tested. The proline residue, at the middle part of the pentapeptide (VPGVG), apparently further disfavors the supramolecular order that is necessary for the formation of the self-assembled nanofibers and the hydrogelation. In addition, according to molecular dynamic studies,<sup>50</sup> VPGVG likely undergoes a conformational transition from an open to a more compact closed state upon an increase in temperature, which results in precipitation of the derivatives of VPGVG (**3F**, **3P**, and **3N**). Compounds **3F**, **3P**, and **3N** all show a dramatic solubility change with pH and exhibit low melting points, agreeing with the fact that the bulky, nonplanar proline residue prevents the efficient molecular packing.<sup>51</sup>

VTEEI, in which the pentapeptide bears two short alkyl side chains and three carboxylic acids, shows the ability to form a

(47) *Solid Phase Synthesis: A Practical Guide*; Kates, S. A., Albericio, F., Eds.; Marcel Dekker: New York, 2000.

(48) Kurkova, D.; Kriz, J.; Rodriguez-Cabello, J. C.; Arias, F. J. *Polym. Int.* **2007**, *56*, 186–194.

(49) Nuhn, H.; Klok, H. A. *Biomacromolecules* **2008**, *9*, 2755–2763.

(50) Glaves, R.; Baer, M.; Schreiner, E.; Stoll, R.; Marx, D. *ChemPhysChem* **2008**, *9*, 2759–2765.

(51) Soto, C.; Sigurdsson, E. M.; Morelli, L.; Kumar, R. A.; Castano, E. M.; Frangione, B. *Nat. Med.* **1998**, *4*, 822–826.

hydrogel over quite a wide range of pH when it attaches to a fluorenyl, pyrenyl, or naphthyl group, suggesting that multiple carboxylic acids, which can serve as both donors and acceptors of hydrogen bonds, facilitate the self-assembly and hydrogelation when there are sufficient hydrophobic interactions originating from the pentapeptides themselves and the aromatic moieties.

Fluorene and naphthalene are appropriate hydrophobic groups to assist the hydrogelation of VYGGG derivatives, but pyrene appears to be too hydrophobic to allow **5P** to dissolve in water even under basic conditions. When the hydrophobic interactions decrease, the pentapeptidic derivatives **5F** and **5N** form hydrogels.

In the case of YGFGG, when phenylalanine replaces one glycine residue in **6P**, proper aromatic–aromatic interaction with the pyrene ring may be allowed, favoring the hydrogelation of **6P** at pH around 5. Compound **6N** shows a gelation ability similar to that of **6P**. Compound **6F** forms a hydrogel at a higher pH (7.8), suggesting efficient aromatic–aromatic interaction in **6F**. To further prove that aromatic–aromatic interaction plays a necessary role for the molecular self-assembly of the pentapeptides in water, we replaced the naphthyl group with a cyclohexyl group to connect to YGFGG or VTEEI at the N-terminal of the pentapeptide. Compounds **4C** and **6C** only afford precipitates (Figure S-1, Supporting Information<sup>46</sup>) and fail to form a hydrogel under the same condition used for **4N** and **6N**, respectively. This result, together with the fact that neither **1N** nor **2N** is a hydrogelator, indicates that adequate aromatic–aromatic interaction is crucial for molecular hydrogelation of these pentapeptide derivatives.

The comparison of the hydrogelators and the properties of the pentapeptide derivative (Table S-1, Supporting Information) suggest several notable trends of the properties of these hydrogelators: (i) The increase of the volume of the alkyl side chains leads to gelation at a relatively high pH. Because all the pentapeptidic derivatives have a free carboxylic acid terminus, a higher pH leads to more deprotonation and results in higher hydrophilicity of the pentapeptidic derivatives. Therefore, the pentapeptides with larger alkyl side chains need a higher pH to achieve sufficient hydrophilicity to balance the increased hydrophobicity caused by the side chains. This trend is also consistent with the calculated log *P* values (Table S-2, Supporting Information). (ii) For the same pentapeptide motif, the derivatives bearing the naphthyl group always form gel under more acidic conditions than those carrying either a fluorenyl or a pyrenyl group, agreeing with the fact that naphthalene provides weaker aromatic–aromatic interaction than the fluorenyl or pyrenyl group does. (iii) The presence of a proline residue in the peptide chain apparently disfavors the molecular self-assembly, likely due to the twisted conformation of proline that restricts this kind of pentapeptide chains to prevent efficient packing between the molecules and hydrogelation. This steric hindrance is amplified when the proline residue closes to the aromatic ring, for example, in compounds **3F**, **3P**, and **3N**, to further destabilize the aromatic–aromatic interactions.

**Fluorescence Emission Spectra.** Although it remains a challenge to determine the precise molecular arrangements of these hydrogelators in the gel phase, the emission spectra of the hydrogelators in the gel and solution phase offer useful and relevant information regarding the interaction of the aromatic rings. Table S-4 (Supporting Information) summarizes the emission peaks in the solution and gel phases of all pentapeptide derivatives that form hydrogels. Emission spectra of the hydrogels (Figure 1) clearly indicate the existence of the excimers of the naphthyl rings, the fluorenyl rings, or the pyrenyl

rings, suggesting that the aromatic–aromatic interactions are pronounced in the corresponding hydrogels. The fluorescence spectra of the hydrogels of **1F** and **6F** exhibit broad peaks at 348 and 365 nm, respectively. The fluorenyl groups in the hydrogel of **1F**, having less sterically hindered side chains than those of other pentapeptides, could stack in a head-to-head manner and also have multiple modes of aromatic–aromatic interactions, which likely contributes to the broadness of its emission peak in the gel phase. The two emission peaks at 344 and 383 nm in the gel phase of **2F** suggest two dominant modes of aromatic–aromatic interactions of fluorenyl groups (likely to be head-to-head and head-to-tail<sup>52</sup>). The hydrogels of **4F** and **5F** exhibit relatively narrow emission peaks at 343 and 346 nm, respectively, suggesting fewer modes of aromatic–aromatic overlap between the fluorenyl groups.

The emission peaks of **1P** at around 453 nm indicate dimerization of pyrenyl groups and suggest efficient aromatic–aromatic interaction between the pyrenyl groups in the hydrogel of **1P**. Other pentapeptide hydrogelators that have the pyrenyl groups also shows peaks around 450 nm in the gel phase and the absence of the same peaks in the corresponding solution phase, indicating the dimerization of pyrene groups in the gel phase. This observation is also consistent with the dimerization of pyrene in other supramolecular hydrogels.<sup>41,53</sup> Generally, there are smaller red shifts in the hydrogels containing fluorenyl or naphthyl groups compared to those containing pyrenyl ones. As shown in Table S-4 (Supporting Information), the red shifts for the hydrogelators containing pyrenyl groups are about 65 nm, and about 55 and around 35 nm for the hydrogelators containing naphthyl groups and fluorenyl groups, respectively.

**Circular Dichroism.** As a helpful tool to determine the secondary structures of proteins, circular dichroism (CD) is useful for assessing the superstructures of these self-assembled pentapeptide derivatives in the gel phase. The differences in the circular dichroism spectra of the gels indicate that even two hydrogels with the same sequence of amino acids can self-assemble in different ways when the hydrophobic groups differ.<sup>46</sup> As shown in Figure 2, **1F** and **1P** share the common feature of  $\beta$ -sheet structure according to the CD spectra. Both of them exhibit a peak near 197 nm ( $\pi\pi^*$  transition) and a trough near 216 nm ( $n\pi^*$  transition), suggesting the backbones of the pentapeptides adopt similar  $\beta$ -sheet-like configurations.<sup>54</sup> The measured CD spectrum of **2F** shows a distinct trough at 205 nm ( $\pi\pi^*$  transition) (characteristic peak of a random coil) and a less pronounced trough at 240 nm ( $n\pi^*$  transition), indicating that it is also contains a  $\beta$ -turn-like arrangement. This observation also resembles the reported results of other short, elastin-like peptides.<sup>49,55</sup> Compound **2P** exhibits weak CD signals, which agrees with the proline residue's poor tendency for self-assembly. Compound **4F** possesses a  $\beta$ -turn structure, characterized by a peak near 218 nm and a trough near 240 nm in its CD spectrum.<sup>56</sup> With a different hydrophobic group attached

(52) Schweitzer, D.; Hausser, K. H.; Haenel, M. W. *Chem. Phys.* **1978**, *29*, 181–185. Channon, K. J.; Devlin, G. L.; Magennis, S. W.; Finlayson, C. E.; Tickler, A. K.; Silva, C.; MacPhee, C. E. *J. Am. Chem. Soc.* **2008**, *130*, 5487–5491.

(53) Tovar, J. D.; Claussen, R. C.; Stupp, S. I. *J. Am. Chem. Soc.* **2005**, *127*, 7337–7345.

(54) Behanna, H. A.; Donners, J.; Gordon, A. C.; Stupp, S. I. *J. Am. Chem. Soc.* **2005**, *127*, 1193–1200.

(55) Reiersen, H.; Clarke, A. R.; Rees, A. R. *J. Mol. Biol.* **1998**, *283*, 255–264.

(56) Ford, S. J.; Wen, Z. Q.; Hecht, L.; Barron, L. D. *Biopolymers* **1994**, *34*, 303–313. Hecht, L.; Barron, L. D. *Faraday Discuss.* **1994**, *99*, 35–47.

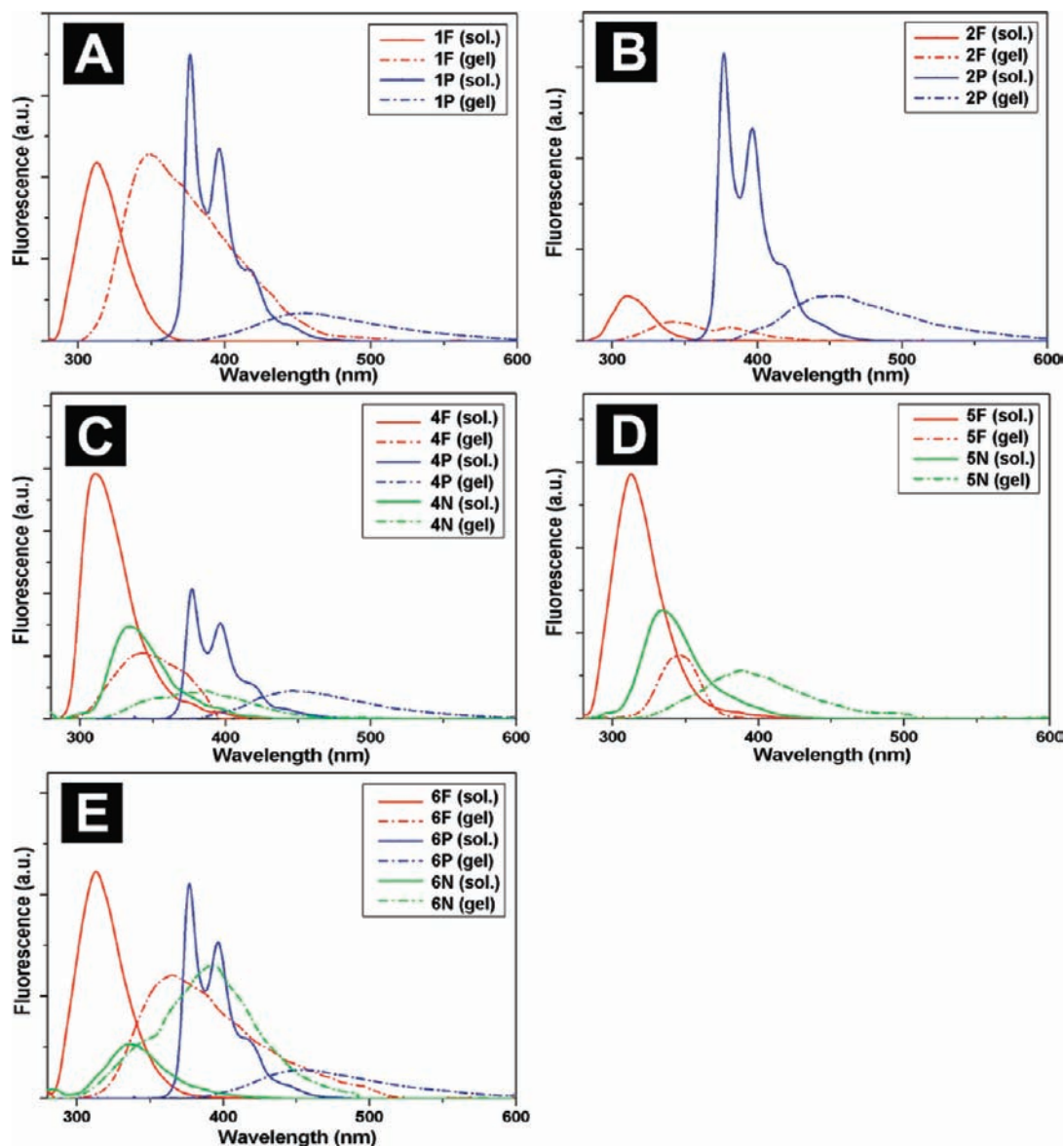


**Figure 1.** Fluorescence spectra of the hydrogels of the pentapeptidic derivatives ( $\lambda_{\text{ex}} = 265, 330, \text{ and } 272 \text{ nm}$  for fluorenyl, pyrenyl, and naphthyl groups, respectively).

to the epitope VTEEI, the CD signals of **4P** suggest more  $\alpha$ -helix rather than  $\beta$ -turn structure. The hydrogel of **4N** only exhibits weak CD signals, suggesting few ordered structures. Compound **5F** shares the common feature of a  $\beta$ -sheet of a polypeptide in the CD signal (below 240 nm), and **5N** exhibits a very weak CD signal. The peak of **5F** arising from 220 nm is due to a peptide  $n\pi^*$  transition, and the trough at 205 nm indicates a less ordered conformation and a characteristic peak of a random coil. As shown in Figure 2E, **6F**, **6P**, and **6N** share similar  $\beta$ -sheet structure.<sup>57</sup> They all have a trough in 217 nm in the CD spectra due to the peptide  $n\pi^*$  transition. The peak near 200 nm with comparable magnitude is due to exciton splitting of the lowest peptide  $\pi\pi^*$  transition. The prominent  $\beta$ -sheet characteristic was observed in the hydrogel of **6N**.

**Microstructures.** According to the SEM and TEM images of the hydrogels, the pentapeptidic hydrogelators self-assemble into nanofibers that physically cross-link to form a fibrous

network as the matrix of the hydrogels. For example, the fibers in **1P** (Figure 3A,B) are short but entangled to form a dense network, which could contribute to its relatively high storage modulus value. The SEM image of **2F** shows flat ribbons (Figure 3C), which could result from the aggregation of the nanofibers of **2F** (Figure 3D). In the SEM image of **2F**, those aggregates of the fibers appear quite random and exhibit a disordered microstructure (Figure 3C), agreeing with the fact that the hydrogel at **2F** lacks thermoreversibility. On the other hand, the cryo-dried hydrogel of **2P** exhibits a quite ordered nanostructure (Figure S-3, Supporting Information<sup>46</sup>) likely due to the dimerization of the pyrenyl group. As shown in Figure 3E,F, the fibrils in the hydrogel of **4P** consist of bundles of the supramolecular chains. Unlike **4F** and **4P**, the fibrils in the hydrogel of **4N** form discrete, short, and coil bundles (Figure S-4F, Supporting Information<sup>46</sup>) after cryo-drying, which could be responsible for its poor mechanical strength and little difference between  $G'$  and  $G''$  in the frequency sweep. As revealed by SEM and TEM of **5F** and **5N**, the fibers of **5F**

(57) Woody, R. W. *Biopolymers* **1969**, *8*, 669. Madison, V.; Schellma, J. *Biopolymers* **1972**, *11*, 1041.



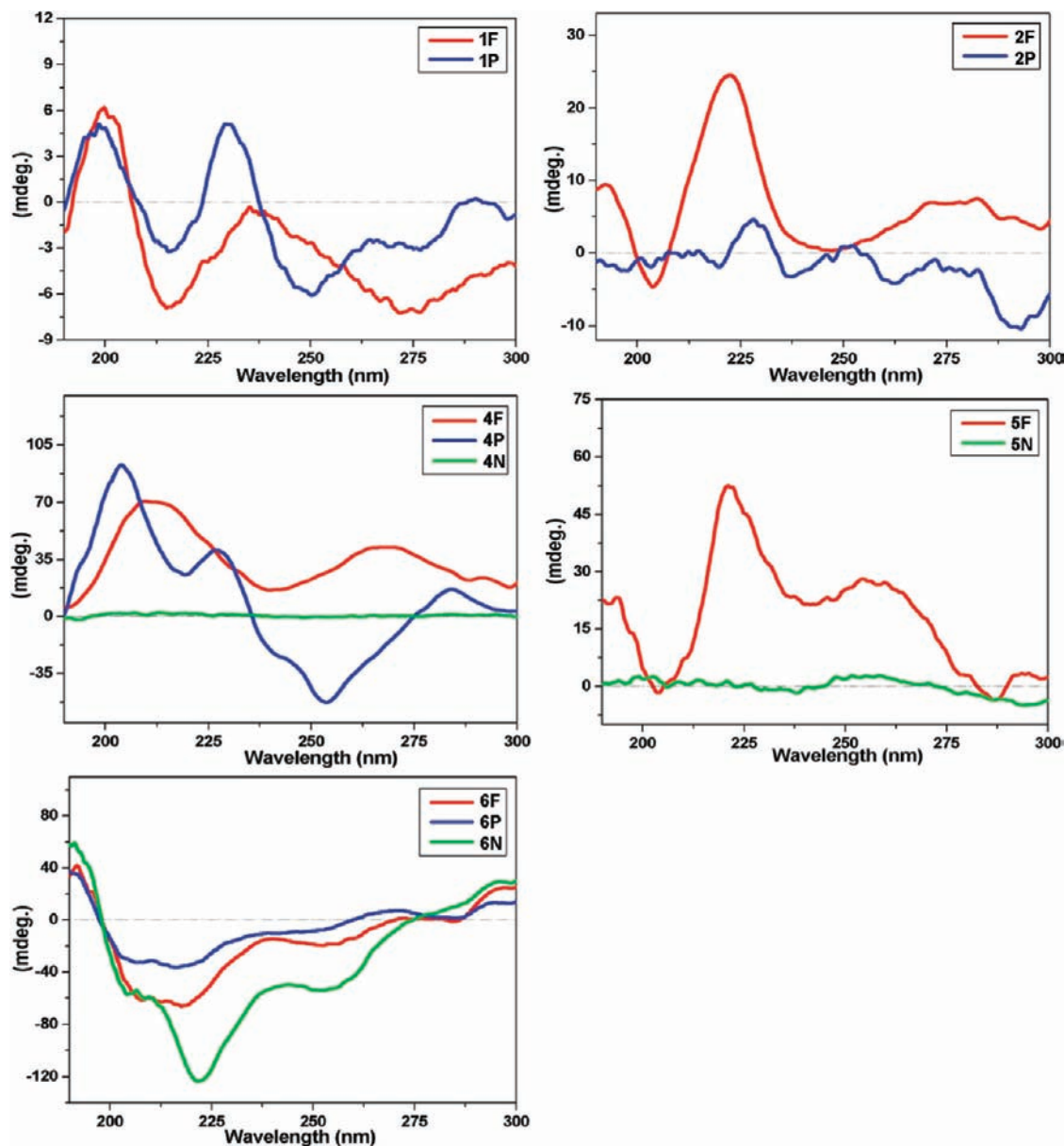


**Figure 2.** CD spectra of the hydrogels formed by the pentapeptidic hydrogelators.

spread out, although some of them randomly aggregate into bundles. The randomness also contributes to the quite scattered fibrous network (Figure 3G). We observed the **5F** gel with a 3D network structure under SEM (Figure 3G), but the TEM image shows an inefficiently cross-linked network (Figure 3H) at a smaller scale. The rheology property also coincides with the TEM image to suggest that **5F** is a weak hydrogelator. In the case of the derivatives of pentapeptide YGFGG, TEM reveals that the three different hydrophobic groups afforded three different kinds of microstructures in their hydrogel matrixes. For example, **6P** seems to self-assemble into short-stick-like microcrystals (Figure 3J) that aggregate randomly to afford a quite irregular packing, as shown in the SEM image (Figure 3I); **6F**, forming the gel at a concentration as low as 1.8 wt %, self-assembles into long and well-organized fibers (Figure S-6, Supporting Information<sup>46</sup>).

**Rheology.** One of the most characteristic properties of gels is their viscoelasticity, which reflects the mechanical properties of the hydrogels. According to the rheological measurement,

the strain sweep and frequency sweep provide sufficient data for studying the deformation and flow of materials, especially in gel states. During strain sweep, the rheological properties of hydrogels are independent of the strain up to a critical strain level. In a frequency sweep, measurements are made at different oscillation frequencies at a constant oscillation amplitude and temperature. As shown in the experimental data of this work, 12 out of the 18 pentapeptide derivatives self-assemble to form the supramolecular hydrogels. To understand their elastic properties, we measured the storage modulus ( $G'$ ) and the loss modulus ( $G''$ ) of these supramolecular hydrogels. All 12 hydrogels studied here show linear viscoelastic responses at strain amplitudes up to 1%. There is a clear domination of  $G'$  over  $G''$  in all 12 hydrogels tested, and in addition, all show negligible frequency dependence. These results should suggest effective and viscoelastic hydrogels. As shown in Table 2, **1P** and **4P** show rather large storage moduli though the concentrations of the peptides in the hydrogels are only 1 and 1.5 wt %, respectively. The storage moduli of **1P** and **4P** are much higher

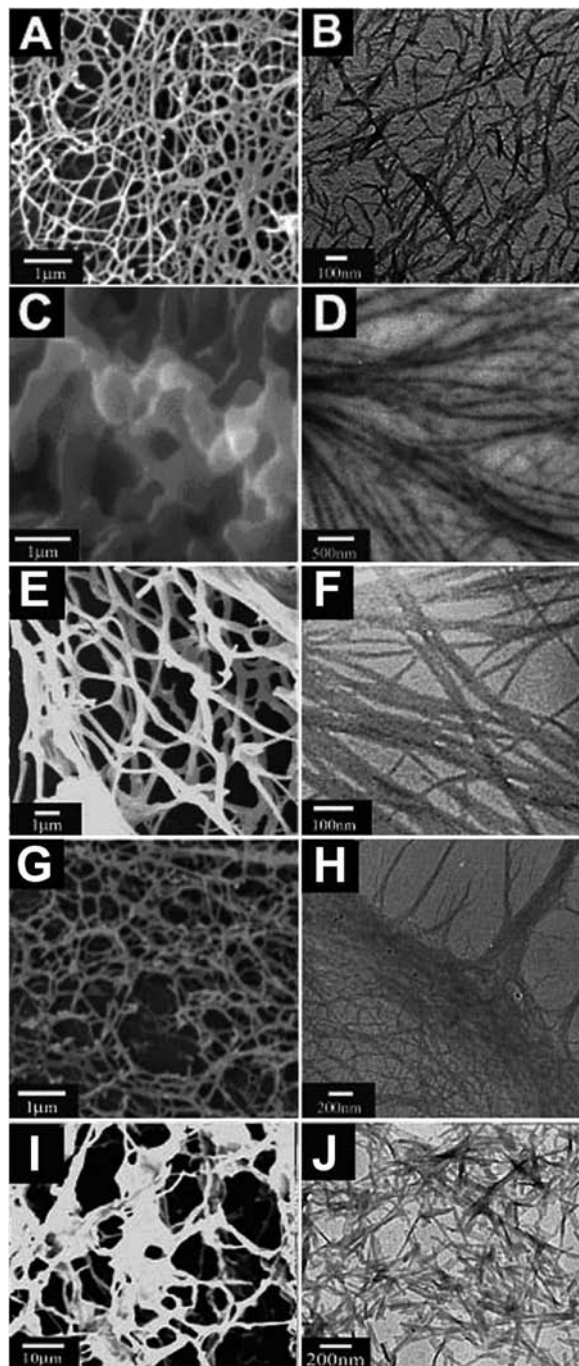


**Figure 3.** Scanning electron micrographs (A, C, E, G, I) and transmission electron micrographs (B, D, F, H, J) of the self-assembled nanofibers in the cryo-dried hydrogels of **1P** (A, B), **2F** (C, D), **4P** (E, F), **5F** (G, H), and **6P** (I, J).

than those of polymeric hydrogels at similar concentration (e.g., the polymeric hydrogels formed by self-assembly of copolypeptides<sup>58</sup> and the cross-linking of peptides<sup>59</sup>). Because of the least steric bulk of the side chains on pentapeptide epitope GAGAS in **1P**, multiple carboxylic acid groups (VTEEI) in **4P**, and the efficient packing via aromatic–aromatic interaction through pyrenyl groups, compounds **1P** and **4P** exhibit excellent

viscoelasticity. Compound **4F** (2.35 wt %) is mechanically stronger than **4N** (1.34 wt %) in terms of viscoelastic behavior, as shown in frequency sweep and strain sweep. Although it forms a clear hydrogel upon heating or changing the pH, **5F** gives a relatively weak elasticity response during the test. In the hydrogel of **6P**, the phenyl ring on the tyrosine or phenylalanine may reduce the probability of the aromatic–aromatic overlap of the pyrenyl group, resulting in a weak viscoelastic property of the gel.

According to the dynamic frequency sweep data, the  $G'$  values of each type of pentapeptide increase in the order of  $F < N < P$ , which follows the extent of the red shifts (nearly constant for **F** (35 nm), **N** (55 nm), and **P** (65 nm)) of the emission spectra of the substituted pentapeptides. This agreement supports the fact that aromatic–aromatic interaction-caused dimerization is an important factor for the mechanical strength of the hydrogels.

**Cytotoxicity Assay.** To verify the biocompatibility of the pentapeptidic derivatives, we use the MTT assay to examine the cell viability after incubating HeLa cells with these pentapeptidic derivatives (Table 3). All the pentapeptides show little cytotoxicity before connecting to the aromatic groups, as indicated by their  $IC_{50}$  values. Among all pyrenyl pentapeptidic derivatives, **1P** and **5P** exhibit lower cytotoxicity than the others. After 3 days of incubation of HeLa cells with GAGAS, **1F**, **1P**, or **1N**, the  $IC_{50}$  of **1P** is 300  $\mu$ M while the  $IC_{50}$  of **1F** and **1N** is 190 and 193  $\mu$ M, respectively, indicating that **1P** is more biocompatible than the derivatives carrying a fluorenyl or naphthyl group. These results suggest that the dimerization of **1P** decreases the cytotoxicity associated with the pyrene motif.

The cytotoxicity of other compounds also supports the above observation. For example, the pyrenyl derivatives of GVGVP and VPGVG show higher cytotoxicity than the other pyrene derivatives (i.e., **4P**, **6P**, and **5P**). According to the result of the MTT assay, **3P** exhibits the highest cytotoxicity, which is consistent with the fact that the proline residue in the middle of the peptide sequence disrupts the dimerization of the pyrenyl group more significantly than in the other cases. These results also agree with the fact that **2P** exists mainly as a monomer at a concentration of 140  $\mu$ M (Figure 4).

In the case of **4P**, the presence of three carboxylic acid groups and one hydroxyl group apparently affects the dimerization of the pyrenyl groups, which makes **4F** or **4N** more biocompatible than the pyrenyl one.

In the case of the hydrogelators derived from VYGGG, the hydrogelators consist of the three smallest amino acids and a tyrosine residue, with the hydrophobic part (VY) at one end and the hydrophilic part (GGG) at the other end. The dimerization of the pyrenyl group and the solubility of the peptide sequence reach an optimal point; therefore, all the derivatives of VYGGG appear to be biocompatible.

In the case of YGFGG, the presence of two hydrophobic and aromatic amino acids (Y, tyrosine; F, phenylalanine) in the epitope YGFGG affects the aromatic–aromatic interaction that is critical for dimerization of the pyrenyl groups. With the presence of valine in the case of **5P**, the glycine residues possess less impact on the aromatic–aromatic interaction of the pyrenyl group than the phenylalanine does in **6P**. The two hydrophobic aromatic parts are separated from Gly; thus, the toxicity of **6P** originates from the dominant monomeric form of **6P** rather than a dimer at 231  $\mu$ M (when compared with **5P**, the most biocompatible one (Figure 4)). Similar to other pyrene-contain-

(58) Nowak, A. P.; Breedveld, V.; Pakstis, L.; Ozbas, B.; Pine, D. J.; Pochan, D.; Deming, T. J. *Nature* **2002**, *417*, 424–428.

(59) Hu, B. H.; Messersmith, P. B. *J. Am. Chem. Soc.* **2003**, *125*, 14298–14299.



**Table 2.** Summary of the Rheological Properties of the Hydrogels

compd	dynamic strain sweep (Pa)		dynamic frequency sweep (Pa)	
	$G'$	$G''$	$G'$	$G''$
1F	224.87 ± 29.74	22.77 ± 1.77	158.22 ± 15.14	12.93 ± 2.93
1P	1600.23 ± 31.02	205.83 ± 16.29	1171.56 ± 19.69	124.09 ± 34.41
2F	196.58 ± 3.10	21.48 ± 1.43	79.80 ± 5.25	12.93 ± 2.93
2P	130.77 ± 8.19	15.47 ± 2.76	20.12 ± 3.16	4.33 ± 1.69
4F	653.79 ± 26.54	113.52 ± 15.15	450.42 ± 62.57	66.71 ± 8.93
4P	20190.24 ± 1172.84	3174.13 ± 389.64	17945.33 ± 580.61	13382.41 ± 239.35
4N	865.16 ± 102.63	133.22 ± 5.48	611.84 ± 89.52	108.37 ± 24.78
5F	93.18 ± 2.98	24.31 ± 2.06	49.32 ± 4.67	31.06 ± 2.45
5N	10.65 ± 1.31	3.24 ± 0.26	8.65 ± 1.31	3.41 ± 0.49
6F	12.73 ± 0.43	3.45 ± 0.22	11.02 ± 1.64	4.06 ± 0.31
6P	14.31 ± 0.52	3.29 ± 0.17	13.63 ± 2.84	3.69 ± 0.41
6N	13.18 ± 0.11	5.58 ± 0.08	8.22 ± 1.87	2.65 ± 0.36

**Table 3.** Summary of the IC<sub>50</sub> Values of All the Compounds against HeLa Cells

	epitope	F	P	N
GAGAS	>1.5 mM <sup>a</sup>	190 μM	300 μM	193 μM
GVGVP	>1.5 mM <sup>a</sup>	>1.5 mM <sup>a</sup>	231 μM	>1.5 mM <sup>a</sup>
VPGVG	>1.5 mM <sup>a</sup>	>1.5 mM <sup>a</sup>	140 μM	>1.5 mM <sup>a</sup>
VTEEI	>1.5 mM <sup>a</sup>	400 μM	160 μM	350 μM
VYGGG	>1.5 mM <sup>a</sup>	>1.5 mM <sup>a</sup>	>1.5 mM <sup>a</sup>	>1.5 mM <sup>a</sup>
YGFGG	>1.5 mM <sup>a</sup>	655 μM	231 μM	445 μM

<sup>a</sup> No toxicity detected at the highest concentration tested (1.5 mM).

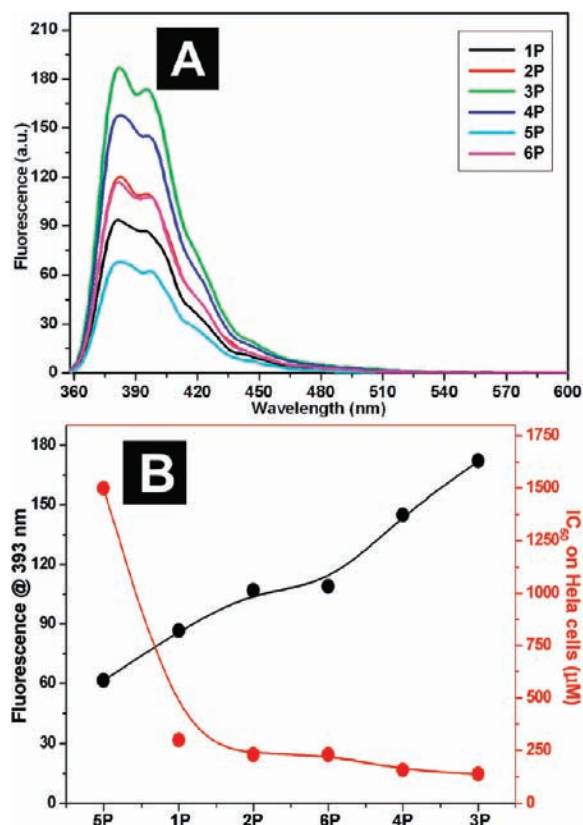


**Figure 4.** (A) Emission spectra of all pyrenyl pentapeptidic derivatives at 140 μM with  $\lambda_{\text{ex}} = 330$  nm. (B) Intensity of the emission at 393 nm and the cytotoxicity of the compounds at 140 μM.

ing pentapeptides, the cytotoxicity of **6P** originates from the monomeric **6P**.

As a general trend observed in this work, the dimerization of pyrenyl groups can improve the biocompatibility of the hydrogelators. The biocompatibility of these pentapeptide-based

hydrogels should be instructive for designing peptide hydrogels as promising nanomaterials for biomedical applications. To further investigate the correlation between dimerization of pyrenyl derivatives and their cytotoxicity, we obtained the emission spectra (Figure 4) of the pyrene derivatives at 140 μM (the lowest concentration for **3P** to exhibit toxicity). Figure 4 indicates that the intensities of the emissions of the monomeric forms follow a decreasing order: **3P** > **4P** > **2P** ≈ **6P** > **1P** > **5P**. This trend matches well with the decrease of the cytotoxicity of those compounds. Compound **5P** shows no toxicity at high concentration (1.5 mM), which has the lowest intensity of emission originating from the monomeric pyrene. The dimerization of pyrene can enhance the biocompatibility of the compounds and minimize the toxicity caused by the pyrene monomer. This result may provide a useful guide to minimize the unintended cytotoxicity of pyrene.

## Conclusion

In summary, we have demonstrated that an aromatic group (fluorenyl, pyrenyl, or naphthyl group), as an effective hydrophobic group and an origin of aromatic–aromatic interaction, brings a powerful driving force for the formation of supramolecular hydrogels. The use of aromatic groups can be a useful alternative to complement the use of alkyl chains, a well-established approach that provides hydrophobic force in the hydrogels of peptide amphiphiles developed by Stupp and co-workers.<sup>60</sup> In addition, the aromatic–aromatic interaction should be useful for developing peptide-based organogels as Banerjee et al. has shown that at least two phenylalanine residues are required for pentapeptide derivatives to form organogels.<sup>61</sup> These results not only provide a starting point and platform to design and study a range of pentapeptide derivatives, but also offer a simple experimental set for potentially developing the theoretical treatment of supramolecular hydrogelation. Although proline-based hydrogelators have been reported,<sup>62</sup> the presence of proline (a well-known  $\beta$ -sheet blocker<sup>63</sup>) between the hydrophilic part strongly affects the noncovalent interaction, which may offer a useful way to refine and control supramolecular interactions within the hydrogels. Although it remains

(60) (a) Hartgerink, J. D.; Beniash, E.; Stupp, S. I. *Proc. Natl. Acad. Sci. U.S.A.* **2002**, *99*, 5133–5138. (b) Palmer, L. C.; Stupp, S. I. *Acc. Chem. Res.* **2008**, *41*, 1674–1684.

(61) Banerjee, A.; Palui, G. *Soft Matter* **2008**, *4*, 1430–1437.

(62) Rodriguez-Llansola, F.; Escuder, B.; Miravet, J. F. *J. Am. Chem. Soc.* **2009**, *131*, 11478–11484.

(63) (a) Chou, P. Y.; Fasman, G. D. *Annu. Rev. Biochem.* **1978**, *47*, 251–276. (b) Wood, S. J.; Wetzel, R.; Martin, J. D.; Hurler, M. R. *Biochemistry* **1995**, *34*, 724–730.

to be verified, this work suggests that the aromatic–aromatic interaction in water may control and assist the formation of hydrogen bonding that is critical for the self-assembly of small molecules in water. The biocompatibility of VYGGG and its derivatives may allow them to serve as hydrogels for tissue engineering. Also, elastin-like hydrogels can potentially serve as attractive building blocks for a range of applications in nanomedicine.

**Acknowledgment.** We acknowledge financial support from the Human Frontier Science Program (HFSP; Grant RGP 0056/2008),

the Hong Kong Research Grant Council (RGC), a start-up grant from Brandeis University, and the NSF (Grant MRSEC 0820492).

**Supporting Information Available:** Abbreviations list, detailed experimental section, synthesis description, and characterization ( $^1\text{H}$  and  $^{13}\text{C}$  NMR, high-resolution mass spectrometry (HRMS), and CD analysis) of the pentapeptidic derivatives. This material is available free of charge via the Internet at <http://pubs.acs.org>.

JA9088764